Shock Wave Properties of Anorthosite and Gabbro

Mark B. Boslough and Thomas J. Ahrens*

Seismological Laboratory, California Institute of Technology, Pasadena, California 91125

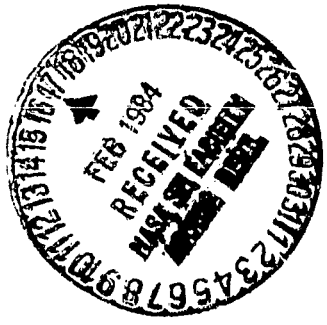

ABSTRACT

Shock wave experiments have been conducted in San Gabriel anorthosite to peak stresses between 5 and 11 GPa using a 40 mm-bore propellant gun. Particle velocity wave profiles were measured directly at several points in each target by means of electromagnetic gauges and Hugoniot states were calculated by determining shock-transit times from the gauge records. The particle velocity profiles yielded sound velocities along the release adiabats which indicate a loss of shear strength upon shock compression for both rocks, with the strength loss persisting upon release to nearly zero stress. Sound velocities of anorthosite shocked to peak stresses between 6 and 10 GPa were measured to be between 5.1 and 5.3 km/s upon release to nearly zero stress. Stress-density release paths in the anorthosite indicate possible transformation of albite to jadeite + (quartz or coesite), with the amount of material transformed increasing from about .4 to .7 mass fraction as the shock stress increased from 6 to 10 GPa shock stress. Electrical interference effects precluded the determination of accurate release paths for San Marcos gabbro. Because of the loss of shear

*now at: Sandia Laboratories, Division 1131, Albuquerque, NM 87185.

strength in the shocked state, the plastic behavior exhibited by anorthosite indicates that calculations of energy partitioning due to impact onto planetary surfaces based on elastic-plastic models may underestimate the amount of internal energy deposited in the impacted surface material.

Introduction

The plagioclase feldspar-bearing rocks anorthosite and gabbro are important components of the lunar and terrestrial crusts. It is necessary to understand the behavior of such rocks under high dynamic stress in order to model cratering processes which result from hypervelocity impacts, and to characterize the stress history of rocks which have been subject to shock loading on planetary surfaces such as the moon and in some meteorites. Shock-wave studies of these and similar materials have been conducted in the past [Ahrens *et al.*, 1969, McQueen *et al.*, 1967, Jeanloz and Ahrens, 1980, Boslough *et al.*, 1983a], but in these studies the data are limited to the Hugoniot state and in some cases a single state on the release isentrope. By employing particle-velocity gauges, a complete stress-strain history subsequent to shock-compression can be determined, along with sound velocity information [Fowles and Williams, 1970, Cowperthwaite and Williams, 1971, Seaman, 1974]. Particle velocity experiments supply detailed release paths, which provide better constraint for mechanical properties and polymorphism than is available with Hugoniot experiments alone.

Peterson *et al.*, [1970] used particle velocity gauges to determine release paths of playa alluvium, tonalite, and novaculite shocked to stresses up to 5 GPa.

They attributed high rarefaction velocities and steep release paths in the stress-density plane to irreversible compaction. Grady *et al.*, [1974] carried out experiments on polycrystalline quartz (novaculite) to 40 GPa using a combination of particle velocity and manganin stress gauges to determine release adiabats and concluded that a partial quartz-stishovite transformation takes place above 15 GPa, with the quantity of material transformed an increasing function of peak stress, and that the Hugoniot states are not on the quartz-stishovite coexistence curve. Similar experiments were conducted on polycrystalline quartz and perthitic feldspar by Grady *et al.*, [1975] and Grady and Murri [1976], who used manganin stress gauges to determine Hugoniot sound velocities, and found that these rocks lose shear strength when shocked to pressures above 20 GPa. Larson and Anderson [1979] used particle velocity gauges to study limestone and tuff at lower stress levels (4 GPa), and attributed the observed time-dependent behavior to the closing of pores in these rocks.

In this paper we present new Hugoniot data on San Gabriel anorthosite and San Marcos gabbro to 11 GPa. Release paths in the stress-density plane and sound velocities are reported, as determined from particle velocity data.

Experimental Methods

San Gabriel anorthosite samples were collected in the San Gabriel Mountains near Pasadena, California. This rock is highly variable in composition and texture and has been studied in detail by Carter [1982]. The particular specimen used in these experiments had randomly oriented plagioclase crystals with a mean grain size of 1-2 mm. Significant alteration was observed at grain boundaries, and the composition is given in Table 1 was determined with a

petrographic microscope. The plagioclase was found to have a mean composition of An_{40} as determined from extinction angle measurements. An electron microprobe analysis indicated a composition of An_{38}.

The San Marcos gabbro was obtained near Escondido, California, and has been studied petrologically by Miller [1937]. Samples from the same specimen used in this study were used in impact and in spall-strength experiments by Lange *et al.*, [1983]. The composition is tabulated in Table 2. Rock samples were cut into 1.5 mm thick, 3.2 by 4.5 cm rectangular slabs, and were bonded together with epoxy, with a U-shaped copper particle-velocity gauge at each interface and one at the free surface. Gauges were photo-etched from 10 μm thick copper foil with a 12.5 μm polyamide (kapton) film backing. Targets were shock-loaded by impact of flat-faced polycarbonate (Lexan) projectiles fired from a 40-mm bore propellant gun at velocities from 1.4 to 2.4 km/s. Projectile velocities were determined using a laser intervalometer [Ahrens *et al.*, 1971].

A uniform magnetic field at right angles to each gauge and to its direction of motion was supplied by a set of Helmholtz coils. An electromotive force V(t) was induced across the gauge element due to its motion through the field

$$V(t) = BLu_p(t) \qquad (1)$$

where B is the magnetic field (≈1.8 kG), L is the effective gauge length (≈1 cm), and $u_p(t)$ is the gauge velocity; equal to the particle velocity of the surrounding medium. These signals were recorded by an array of cathode ray oscilloscopes. The experiment is shown schematically in Fig. 1 and described in detail by Boslough [1983].

The geometry and time history of a typical experiment is illustrated by means of an x-t diagram in Fig. 2. The stationary rock target lies to the right of the origin, with four particle velocity gauges initially at intervals of 1.5 mm. The polycarbonate projectile approaches from the left and strikes the x=0 surface of the target at time t=0, driving a shock wave to the right into the rock and to the left into the projectile. Each gauge is stationary until overtaken from the left by the shock wave, at which time it begins moving with the particle velocity associated with the Hugoniot state. The shock wave reflects from the free surface as a rarefaction wave, and each gauge again accelerates to the right as this wave passes through it from the right.

Results

Typical particle velocity records for shocked anorthosite and gabbro are shown in Fig. 3. The sudden increase corresponds to shock wave arrival, and the second increase corresponds to the acceleration from free-surface rarefaction. The gabbro records were found to be significantly noisier than the anorthosite records in all cases. This was presumed to result from the presence of piezoelectric quartz grains in the gabbro, whereas the anorthosite was relatively free of quartz.

Digitized oscilloscope records for anorthosite shocked to 10 GPa are shown in Fig. 4. Synchronization of the four signals in time was achieved by means of a fiducial pulse received simultaneously at each oscilloscope. Shock-transit times were taken from the interval between arrival at different gauges and were used to determine shock velocity. The known projectile velocity and polycarbonate Hugoniot [Marsh, 1980] were used with an impedance-match solution [McQueen

et al., 1970] to determine the Hugoniot states achieved in the rocks. Eulerian sound velocities were determined from the transit time of the free-surface rarefaction front and the Hugoniot density. Hugoniot states and sound velocities for both rocks are given in Tables 3 and 4.

The observed release waves are nonsteady simple waves and can be inverted to stress-density release paths by numerically integrating the equations for conservation of mass and linear momentum [Cowperthwaite and Williams, 1971]

$$\left(\frac{\partial \rho}{\partial u_p}\right)_h = \frac{\rho^2}{\rho_o C(u_p)} \tag{2}$$

$$\left(\frac{\partial \sigma}{\partial u_p}\right)_h = \rho_o C(u_p) \tag{3}$$

where ρ is the density, ρ_o is the initial density, σ is the stress, u_p is the particle velocity, and h is the Lagrangian space coordinate along the direction of wave propagation. The Lagrangian sound velocity is determined by the finite difference approximation

$$C(u_p) \approx \frac{\Delta h}{\Delta t} \tag{4}$$

where Δh is the initial distance between gauges and Δt is the transit time for a disturbance with particle velocity u_p. In the case of anorthosite, the release paths are smooth and single-valued (Fig. 3a). The oscilloscope records were digitized and integrated directly. The resulting release paths are consistent, and are plotted in Fig. 5. Because of the noisiness of the gabbro records (Fig. 3b), it was necessary to approximate the rarefaction waves by smooth curves before integrating. Complete release paths were not obtained, and the partial

release paths are less consistent than those of anorthosite. Eulerian sound speeds, equal to $\frac{\rho_o}{\rho} C(u_p)$, were also calculated for the release paths in both rocks. These are plotted as a function of stress in Fig. 7.

Discussion

Sound velocities of anorthosite from this study can be compared to those measured ultrasonically for anorthosite rocks of similar composition [Birch, 1960, Birch, 1961, Simmons, 1964, Anderson and Liebermann, 1968, Liebermann and Ringwood, 1976]. At T = 25°C and P > 0.4 GPa, longitudinal velocities have been measured in anorthosite with composition between An_{49} and An_{56} in the range $6.76 \geq v_p \geq 7.47$ km/sec, and shear velocities in the range $3.87 \leq v_s \leq 4.09$ km/sec. Bulk sound velocities,

$$v_\phi^2 = v_p^2 - \frac{4}{3} v_s^2 \qquad (5)$$

are therefore in the range $5.04 \leq v_\phi \leq 5.99$ km/sec. Fig. 4-6 demonstrates that in all three shock wave experiments, the sound velocity approaches 5.2 km/sec as the rock releases to zero pressure, indicating a loss of shear strength upon shock compression which is never regained. This is analogous to observations by Grady *et al.*. [1975] for polycrystalline quartz, where the loss of strength in that material was attributed to heterogeneous partitioning of shock energy into "shear bands" in which melting occurs. Optical observations consistent with this theory have been made for various minerals by Kondo and Ahrens [1983], and for anorthite glass by Schmitt and Ahrens [1983b].

Not as clear a case can be made for the loss of shear strength in gabbro, due to the lower quality of the data. However, in most of the experiments the measured sound velocities are consistently lower for the gabbro than for the anorthosite.

Release paths for anorthosite, illustrated in Fig. 5, are significantly steeper than the Hugoniot. Similar release behavior was observed in anorthite glass (initial density = 2.69 Mg/m^3) by Boslough *et al.* [1983b]. The reason for the densification of the glass upon release was attributed to irreversible compaction or annealling of the amorphous material behind the shock wave to a denser form. Partial release paths can be extrapolated to the anorthite single crystal density of 2.76 Mg/m^3. This argument cannot be used to explain the release behavior of anorthosite, however. The phase transformation: $NaAlSi_3O_8$ (albite) → $NaAlSi_2O_6$ (jadeite) + SiO_2 (quartz or coesite) is a more reasonable explanation, particularly in light of the identification of shock-induced formation of jadeite from oligoclase in material from the Ries Crater in Germany [James, 1969]. The assemblage $(anorthite)_{38}$ + $(jadeite + quartz)_{62}$ has a density of 3.01 Mg/cm^3, and $(anorthite)_{38}$ + $(jadeite + coesite)_{62}$ has a density of 3.06 Mg/cm^3. At 293°K, $NaAlSi_2O_6 + SiO_2$ are the stable phases above 0.6 GPa [Clark, 1966]. The present experiments are well above the transformation pressure, so the only barriers to the phase transition are kinetic. The zero pressure density of the released anorthosite can be used to estimate the amount of material transformed. For example, the final densities are in the range 2.72 to 2.79 Mg/m^3 which requires the transformation of from 42 to 73 % of the albite to high pressure phases. The possibility of pore-space crushing and irreversible compaction would bring this estimate down somewhat. It is clear from the data

that the fraction of albite transformed to high pressure phases is an increasing function of peak stress. This result is analogous to the conclusion of Grady *et al.*, [1974] for higher pressures that the release path of shocked polycrystalline quartz is controlled by the quartz → stishovite transition. The release data for gabbro, are not of good enough quality to resolve whether the release paths are above or below the Hugoniot.

Conclusions

Because the unloading wave speed approaches the bulk sound speed, we conclude that San Gabriel anorthosite loses shear strength upon shock compression to pressures greater than 6 GPa. Because strength effects can probably be neglected in this material, its release behavior can be attributed to the phase transformation of albite to jadeite and quartz or coesite. The amount of material transformed is likely to be controlled by kinetics, and appears to be an increasing function of shock pressure. This may be due to the localization of shock heating into shear bands, in which the temperature is high enough for the phase transition to occur. The mechanical result of the shear banding is hypothesized to be fluid-like rheological behavior upon release [Grady et al., 1975, Grady, 1980]. The hydrodynamic behavior of shocked anorthosite will result in less rapid attenuation of a decaying shock wave than obtained in the usual elastic plastic rheological model.

In calculations by O'Keefe and Ahrens [1977] of energy partitioning of a hypervelocity impact onto the anorthosite surface of a planet, the release behavior of the rock was assumed to be elastic-plastic [Fowles, 1960, Davison and Graham, 1979]. This assumption would overestimate the attenuation of the

shock wave due to catch-up of the rarefaction wave from the free surface of the impacting body. Thus, a larger quantity of surface material is shocked above a given pressure, and estimates by O'Keefe and Ahrens [1977] of the fraction of meteoroid kinetic energy deposited in the planetary surface material will be too low.

Acknowledgements

We appreciate the assistance of E. Gelle, W. Ginn, J. Long, and M. Long in building and carrying out experiments. We thank R. Heuser, R. Hill, and S. Rigden for analyzing rock samples, and S. Sondergaard for help in fabricating gauges. This work was supported under NASA Grant NGL 05-002-105. Contribution 4013, Division of Geological and Planetary Sciences, Pasadena, California 91125.

References

Ahrens, T.J., C.F. Petersen, and J.T. Rosenberg. Shock compression of feldspars. *J. Geophys. Res.*, *74*, 2727-2746,1969.

Ahrens, T.J., J.H. Lower, and P.L. Lagus, Equation of state of fosterite, *J. Geophys. Res.*, *76*, 518:528,1971

Anderson, O. L., and R. C. Liebermann, Sound velocities in rocks and minerals; experimental methods, extrapolations to very high pressures, results, in: *Physical Acoustics IVB*, edited by W P. Mason, pp. 330-472, Academic Press, New York, 1968.

Birch, F., The velocity of compressional waves in rocks to 10 kilobars, 1, *J. Geophys. Res.*, *45*, 1083-1102, 1960.

Birch, F., The velocity of compressional waves in rocks to 10 kilobars,2, *J. Geophys. Res.*, *66*, 2199-2224,1961.

Boslough, M. B., *Shock Wave Properties and High-Pressure Equations of State of Geophysically Important Materials*, Ph.D. Thesis, California Institute of Technology, Pasadena, CA, 1983.

Boslough, M. B., Ahrens, T. J., & Mitchell, A. C., Shock temperatures in anorthite glass, *Geophys. J. R. astr. Soc.*, submitted, 1983a.

Boslough, M. B., Rigden, S. M., & Ahrens, T. J., Hugoniot equation of state of anorthite glass and lunar anorthosite, *Geophys. J. R. astr. Soc.*, submitted, 1983b.

Carter, B. A., Field petrology and structural development of the San Gabriel

Excursion in the Transverse Ranges, edited by J. D. Cooper, pp. 1-47, Geological Society of America, 1982.

Clark, S. P., Jr., High-pressure phase equilibria, in: *Handbook of Physical Constants*, edited by S. P. Clark, Jr., pp. 345-883, Geological of America, New York, 1966.

Cowperthwaite, M., and R. F. Williams, Determination of constitutive relationships with multiple gages in nondivergent flow, *F. Appl. Phys.*, *42* , 456-462, 1971.

Davison, L. and R. A. Graham, Shock compression of solids, *Physics Reports*, *55* , 255-379, 1979.

Dremin, A. N., and K. K. Shvedov, The determination of Chapman-Jouguet pressure and of the duration of reaction in the detonation wave of high explosives, *Zh. Prikl, Mekh. Tekh. Fiz.*, **2** , 154-159, 1964.

Fowles, G. R., Attenuation of the shock wave produced in a solid by a flying plate, *J. Appl. Phys.*, *31* , 655-661, 1960.

Fowles, R., and R. F. Williams, Plane stress wave propagation in solids, *J. Appl. Phys.*, *41* , 360-363, 1970.

Grady, D. E., W. J. Murri, and G. R. Fowles, Quartz to Stishovite: wave propagation in the mixed phase region, *J. Geophys. Res.*, *79* , 332-338, 1974.

Grady, D. E., W. J. Murri, and P. DeCarli, Hugoniot sound velocities and phase transformations in two silicates, *J. Geophys. Res.*, *80* , 4857-4861, 1975.

Grady, D. E., and W. J. Murri, Dynamic unloading in shock compressed feldspar, *Geophys. Res. Lett.*, 472-474, 1976.

Grady, D. E., Shock deformation of brittle solids, *J. Geophys. Res. 85*, 913-914, 1980.

James, O. B., Jadeite: shock-induced formation from oligoclase, Ries Crater, Germany, *Science, 165*, 1005-1008, 1969.

Jeanloz, R. and T. J. Ahrens, Anorthite: Thermal equation of state to high pressures, *Geophys. J. R. astr. Soc., 62*, 529-549, 1980.

Kondo, K. and T. J. Ahrens, Heterogeneous shock-induced thermal radiation in minerals, *Phys, Chem. Minerals, 9*, 173-181, 1983.

Lange, M., T. J. Ahrens, and M. B. Boslough, Impact cratering and spall fracture of gabbro, Icarus, submitted, 1983.

Larson, D. B. and G. D. Anderson, Plane shock wave studies of porous geologic media, *J. Geophys. Res., 84*, 4592-4600, 1979.

Liebermann, R. C., and A. E. Ringwood, Elastic properties of anorthite and the nature of the lunar crust, *Earth Planet. Sci. Lett., 31*, 69-74, 1976.

Marsh, S. P., *LASL Shock Hugoniot Date*, 680 pp. University of California Press, Berkeley, 1980.

McQueen, R. G., S. P. Marsh, and J. N. Fritz, Hugoniot equation of state of twelve rocks, *J. Geophys. Res., 72*, 4999-5936, 1967.

McQueen, R. G., S. P. Marsh, J. W. Taylor, J. N. Fritz, and W. J. Carter, The equation of state of solids from shock-wave studies, in R. Kinslow, *High Velocity Impact Phenomena*, Academic Press, 294-419.

Miller, F. S., Petrology of the San Marcos gabbro, Southern California, *Bull.*

Geol. Soc. Amer., *48*, 1397-1426, 1937.

O'Keefe, J. D. and T. J. Ahrens, Impact-induced energy partioning, melting, and vaporization on terrestrial planets, *Proc. Lunar Sci. Conf. 8th*, 3357-3374, 1977.

Peterson, C. F., W. J. Murri, and M. Cowperthwaite, Hugoniot and release-adiabat measurements for selected geologic materials, *J. Geophys. Res.*, *75*, 2063-2072, 1970.

Schmitt, D. R. and T. J. Ahrens, Temperatures of shock-induced shear instabilities and their relationship to fusion curves, *Geophys. Res. Lett.*, *10*, no. 11, 1077-1080, 1983.

Seaman, L., Lagrangian analysis for multiple stress or velocity gages in attenuating waves, *J. Appl. Phys.*, *45*, 4303-4314, 1974.

Simmons, G., Velocity of shear waves in rocks to 10 kilobars, 1, *Geophys. Res.*, *69*, 1123-1130, 1964.

Figure Captions

Fig. 1. Schematic drawing of particle velocity experiment, with major components indicated: A. Polycarbonate projectile, B. 40 mm-bore gun barrel, C. Timing laser, D. Photodetector, E. High-power switch (ignitron), F. Capacitor bank, G. Helmholtz coils, H. Rock target, I. Self-shorting trigger pins, J. Fiducial pulse generator, K. Copper foil particle velocity gauge elements.

Fig. 2. Particle velocity experiment represented by x-t diagram. Projectile approaches stationary target from left and impacts at t=0.

Fig. 3. Oscillograms of particle velocity-time profiles in (a) anorthosite and (b) gabbro. Gabbro signals are significantly noisier, presumably due to presence of quartz grains.

Fig. 4. Digitized particle velocity gauge records from experiment 40-571 in which anorthite was shocked to 10 GPa.

Fig. 5. Hugoniot states and release paths of San Gabriel anorthosite. Included are two Hugoniot states of anorthite glass [Boslough et al., 1983], with respective partial release states.

Fig. 6. Hugoniot states and partial release paths of San Marcos gabbro. Noisy particle velocity records precluded determination of release to zero stress.

Fig. 7. Eulerian sound speeds along release paths of shocked San Gabriel anorthosite. Hatched region indicates range of possible zero pressure bulk sound velocities.

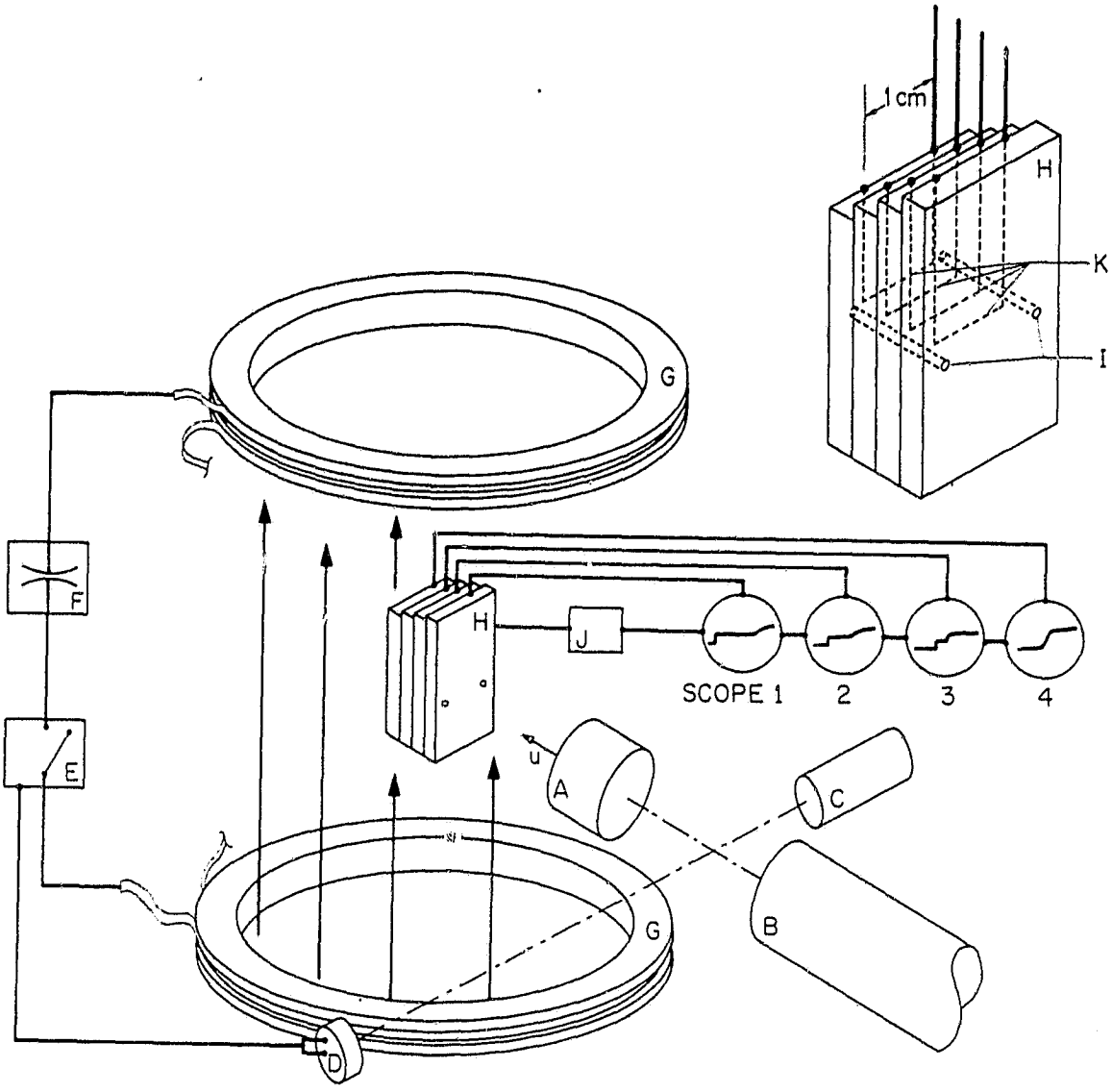

TJA83132SFD

Fig. 1

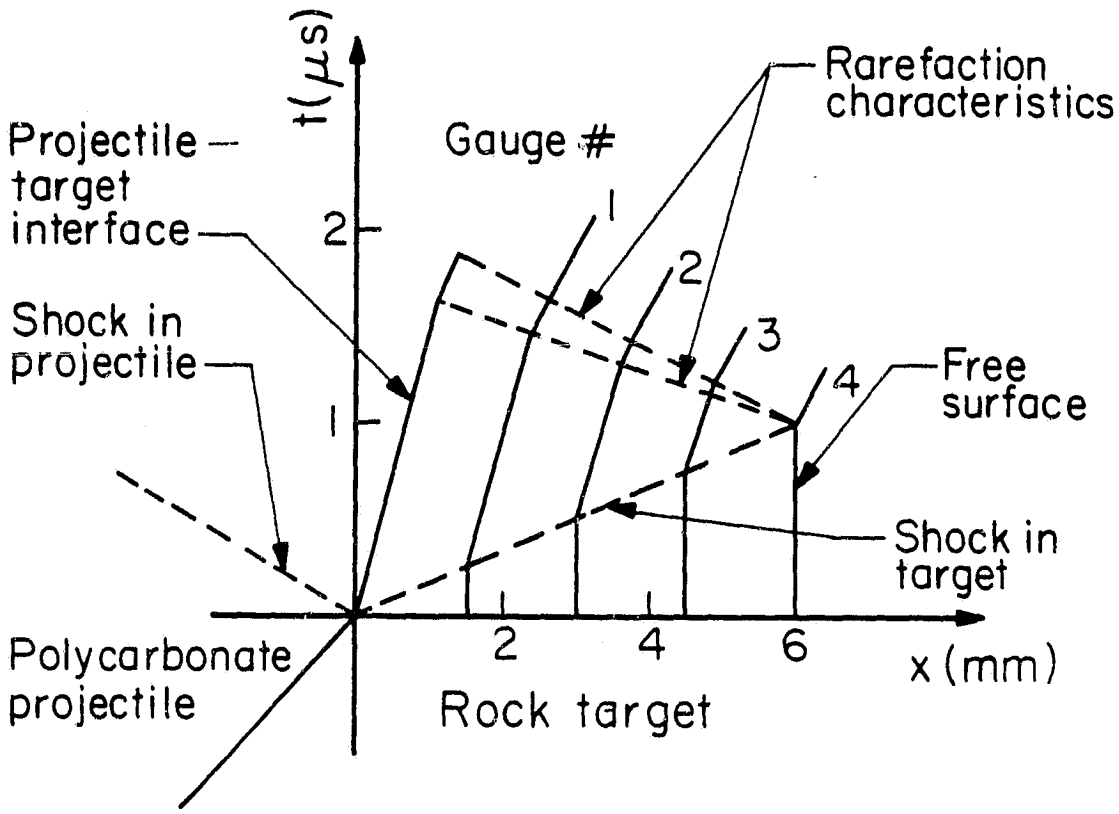

TJA83133SFD

Fig. 2

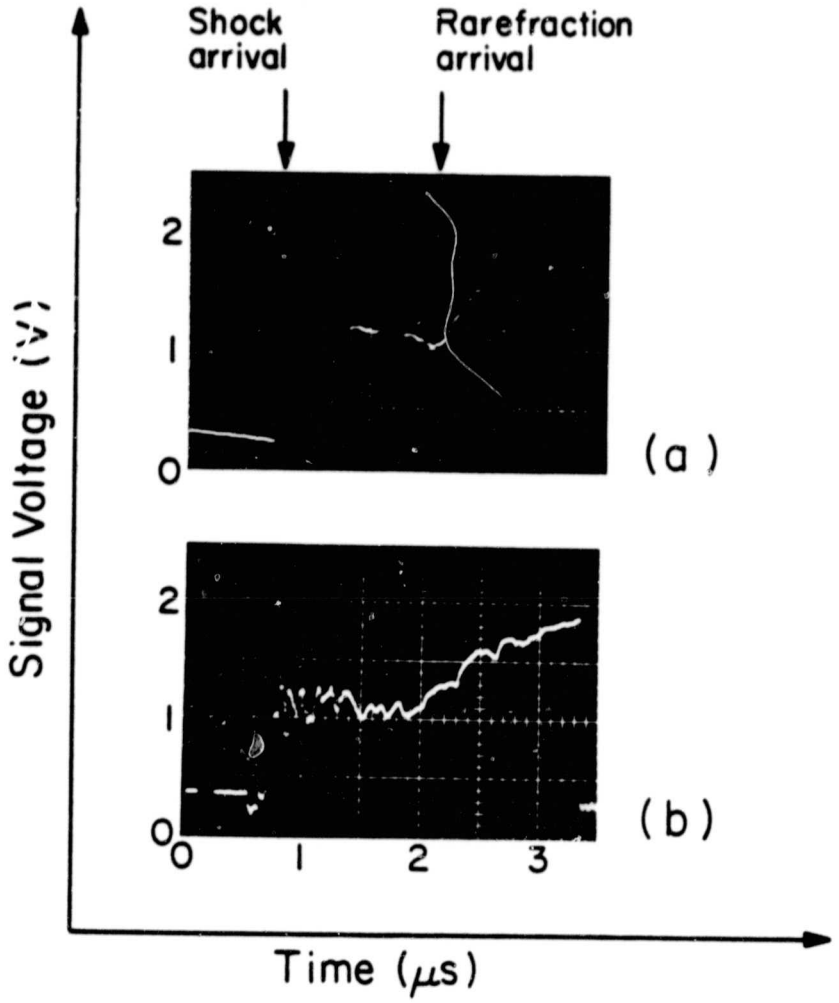

Fig. 3

TJA83134SFD

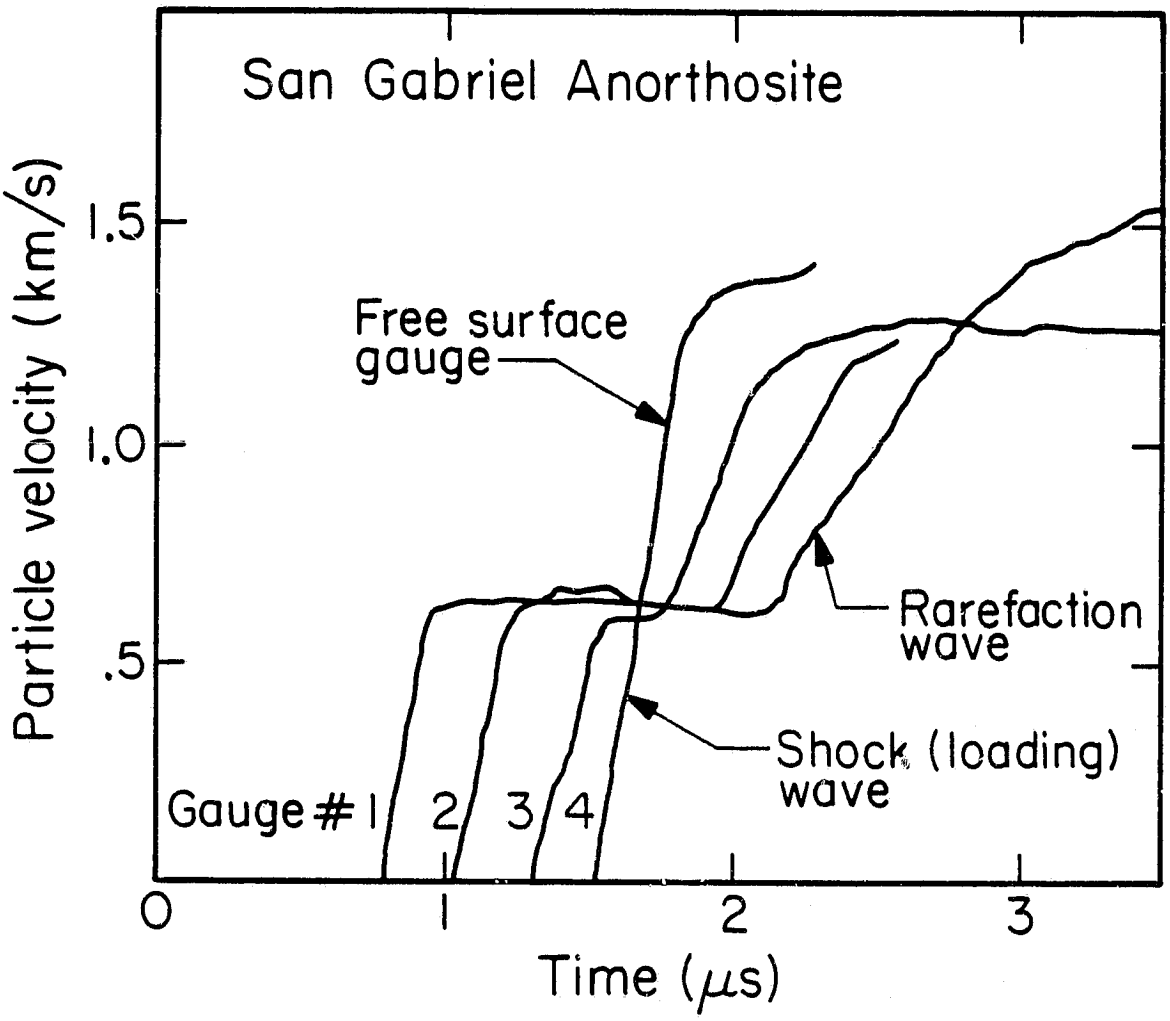

TJA83135SFD

Fig. 4

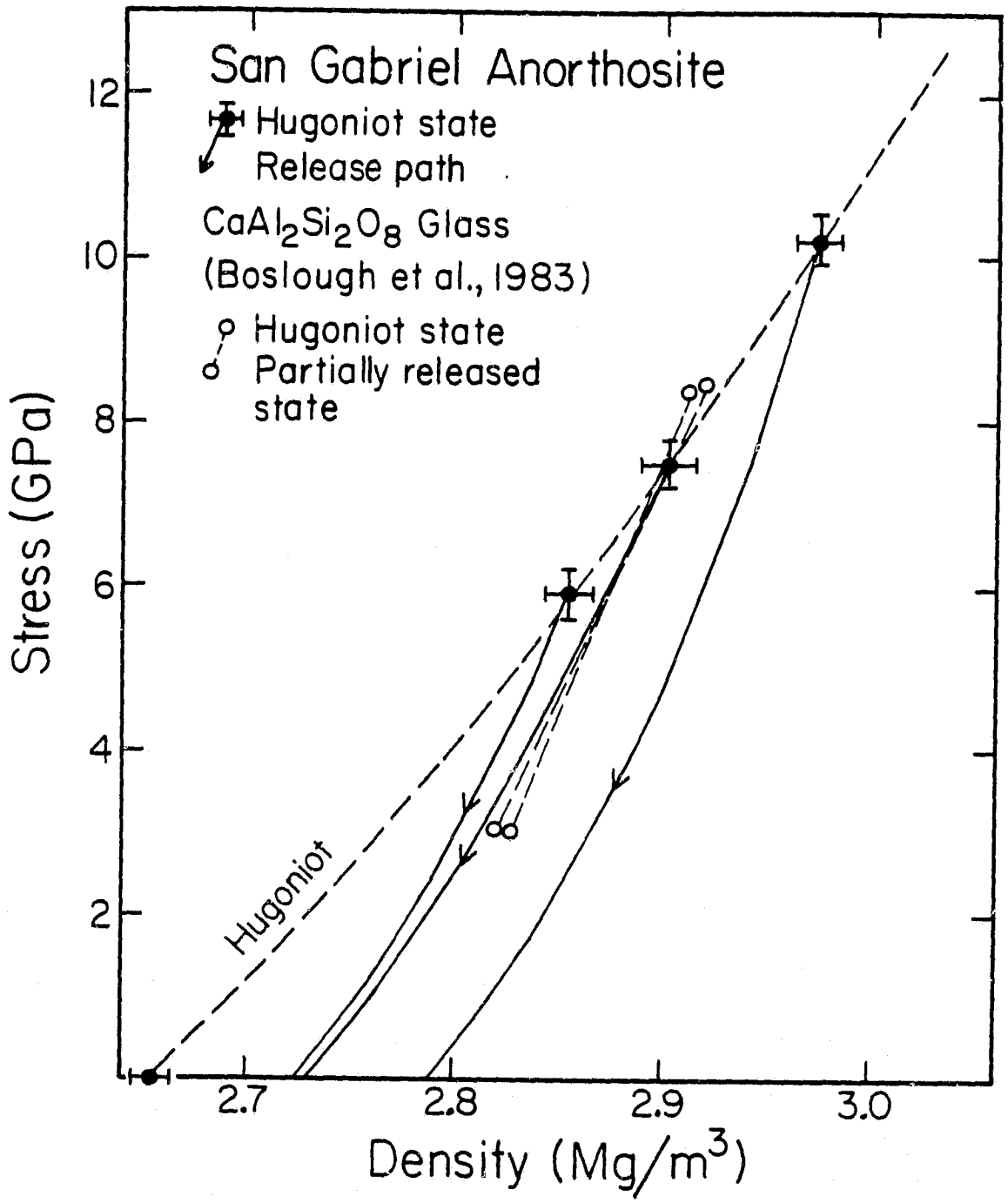

Fig. 5

TJA83136SFD

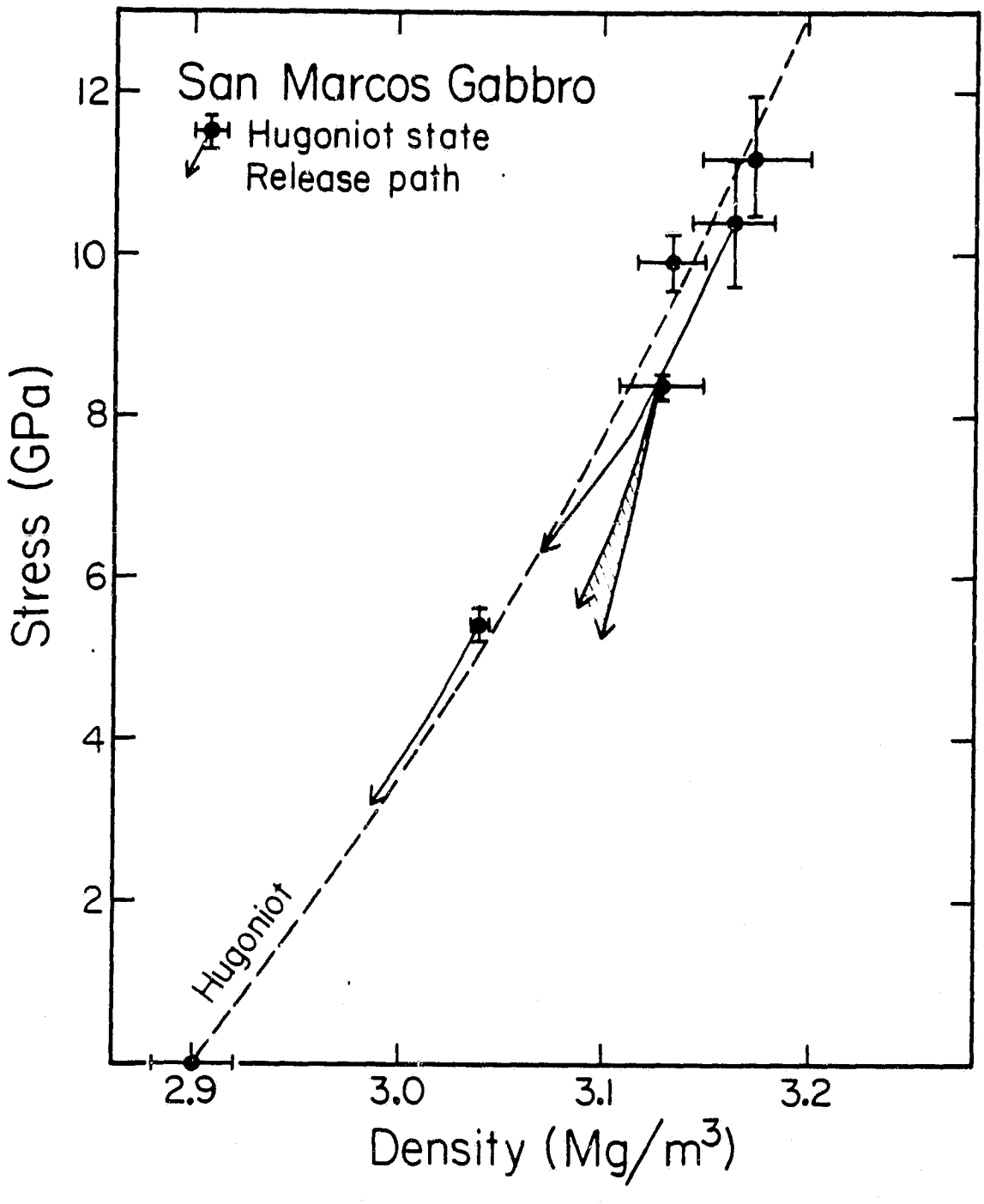

Fig. 6

TJA83137SFD

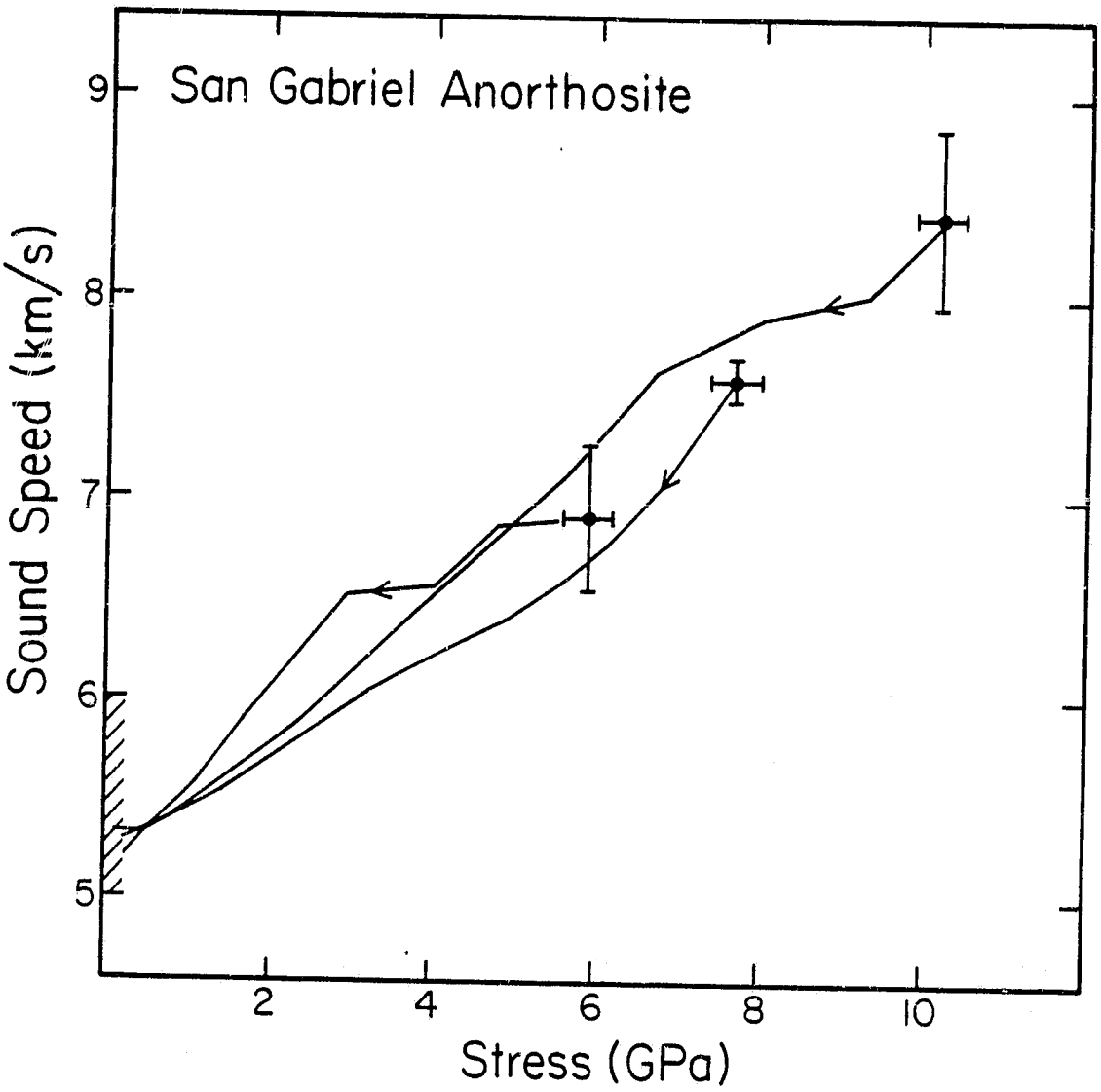

TJA83138SFD

Fig. 7

Table 1

San Gabriel Anorthosite Composition

Mineral	Volume %
Plagioclase *	91
White Mica	6
Epidote	3
Opaques	trace
Quartz	trace
Apatite	trace

* An_{40}

(Analysis by S. Rigden)

Table 2

San Marcos Gabbro Composition

Mineral	Volume %
Plagioclase	67.9
Amphibole	22.5
Clinopyroxene	1.5
Orthopyroxene	1.1
Quartz	1.4
Biotite	0.9
Opaques	4.3
Alakali feldspar	trace
Calcite	trace
Chlorite	trace
Apatite	trace

(Analysis by R. Hill)

Table 3

San Gabriel Anorthosite Shock Wave Data

Shot	Projectile Velocity (km/s)	Initial Density (Mg/m^3)	Shock Velocity (km/s)	Particle Velocity (km/s)	Pressure (GPa)	Density (Mg/m^3)	Sound Velocity (km/s)
40-572	1.575 ±.050	2.656 ±.013	5.648 ±.055	.394 ±.022	5.91 ±.31	2.855 ±.011	6.90 ±.36
40-570	1.881 ±.050	2.653 ±.007	5.725 ±.117	.493 ±.020	7.47 ±.28	2.903 ±.014	7.59 ±.10
40-571	2.351 ±.050	2.653 ±.007	5.985 ±.032	.644 ±.020	10.23 ±.30	2.973 ±.011	8.39 ±.44

Table 4

San Marcos Gabbro Shock Wave Data

Shot	Projectile Velocity (km/s)	Initial Density (Mg/m^3)	Shock Velocity (km/s)	Particle Velocity (km/s)	Pressure (GPa)	Density (Mg/m^3)	Sound Velocity (km/s)
40-569	1.394 ±.009	2.907 ±.008	6.487 ±.035	.286 ±.011	5.39 ±.20	3.041 ±.004	6.5 ±.1
40-573	1.968 ±.008	2.886 ±.001	6.11 ±.30	.474 ±.016	8.36 ±.14	3.129 ±.022	8.5 ±.4
40-555	2.187 ±.050	2.892 ±.007	6.66 ±.19	.515 ±.020	9.91 ±.34	3.135 ±.015	--- ---
40-556	2.242 ±.032	2.929 ±.039	6.898 ±.042	.515 ±.048	10.41 ±.0.84	3.165 ±.020	7.0 ±.5
40-574	2.418 ±.025	2.874 ±.049	6.404 ±.016	.608 ±.052	11.19 ±.77	3.176 ±.026	6.7 ±.5